-RESEARCH PAPER-

International Journal of Mining and Geo-Engineering

IJMGE

IJMGE 59-3 (2025) 281-297

DOI: 10.22059/IJMGE.2025.393902.595243

Comparison of optimizers (Adam, RMSprop, SGD and Adagrad) in a neural network for mineral resource classification: a case study in a copper deposit in Peru

Marco Antonio Cotrina-Teatino [a, *], Jairo Jhonatan Marquina-Araujo [a], Jose Nestor Mamani-Quispe [b] and Solio Marino Arango-Retamozo[a]

[a] *Department of Mining Engineering, Faculty of Engineering, National University of Trujillo, Trujillo, Perú.*

[b] *Faculty of Chemical Engineering, National University of the Altiplano, Puno, Perú.*

Article History:

Received: 22 April 2025.

Revised: 27 May 2025.

Accepted: 27 July 2025.

ABSTRACT

This study has compared the performance of various optimizers in mineral resource classification using a multilayer perceptron artificial neural network (MLP) applied to a copper deposit in Peru. The optimizers Adam (Adaptive moment estimation), RMSprop (Root mean square propagation), SGD (Stochastic gradient descent), and Adagrad (Adaptive gradient algorithm) were evaluated to assess their impact on the spatial continuity of block classification. A total of 318,443 blocks were estimated using ordinary kriging, based on key variables including estimated grade, kriging variance, average sample distance, number of composited samples, the kriging Lagrangian, and geological confidence. The methodology involved a mixed multivariable block-by-block clustering using the k-prototypes algorithm, followed by block smoothing through an artificial neural network with different optimizers. Results show that the Adam optimizer achieved the highest overall accuracy (93%), outperforming both RMSprop and SGD (92%), as well as Adagrad (90%). In addition, Adam yielded a more homogeneous classification of mineral resources. It categorized 75,869 blocks as measured (1,395.99 Mt total tonnage, 5.40 Mt fine copper), 120,039 as indicated (2,208.72 Mt and 6.56 Mt fine copper), and 122,535 as inferred (2,254.64 Mt and 6.29 Mt fine copper). In conclusion, the model trained with the Adam optimizer demonstrated superior precision and stability in mineral resource classification, effectively mitigating the "spotty dog effect" and improving the geological coherence of the block model.

Keywords: *Mineral resource classification, Artificial neural network, ANN optimizers, K-Prototypes clustering, Geostatistics.*

1. Introduction

Mineral resources are a fundamental pillar for the development and sustainability of modern civilization [1, 2]. Their significance is evident across multiple sectors, including socioeconomic growth, industrial production, advanced technology manufacturing, and transportation infrastructure [2–4]. A mineral resource is defined as "a concentration of natural material in or on the Earth's crust, in such form and quantity that its extraction is currently or potentially economically feasible" [5–7]. Mineral resources are categorized into three classes, Inferred, Indicated, and Measured based on the degree of geological confidence and available data (Figure 1) [7]. This classification of mineral resources subsequently leads to the classification of mineral reserves, which aims to quantify the tonnage and average grade of the deposit based on economic and technological criteria that ensure its feasibility for exploitation [8]. Mineral reserves are further subdivided into two categories: Probable and Proved [9–11].

The classification of mineral resources is a fundamental process in mining exploration projects, particularly in feasibility studies, as it allows for the assessment of uncertainty and risk associated with mineral deposit estimation. At this stage, geostatistical methods play a crucial role by providing tools to quantify spatial variability and improve the reliability of resource classification. Key criteria used in classification include drill hole spacing, kriging variance, multi-pass kriging schemes, and uncertainty models derived from geostatistical simulations [12–21]. The accuracy of this classification directly impacts various subsequent stages of the mining project, as key parameters, such as mineral tonnage and cutoff grade are dependent on the robustness of the classification process [14, 22].

The assignment of resource categories is carried out by a Qualified Person (QP), who must consider multiple factors to ensure the reliability of the classification. These factors include confidence in the geological model, spatial characteristics of the deposit, such as grade continuity and mineralized domains, data density, and results from the analytical quality control program, all of which are essential for assessing the accuracy of the estimation method [9, 23, 24]. While some of these aspects are qualitative and require geological interpretation, others can be quantified using numerical models to establish the confidence level in the estimation [25, 26].

The classification of mineral resources requires the consideration of multiple variables, many of which have been extensively studied in literature. According to Cevik et al. [25], the most relevant variables in this process (commonly referred to as "features" in machine learning) include: (i) the geological domain in which the block is located, (ii) kriging variance, (iii) the coefficient of variation of the estimation, (iv) the kriging pass, (v) the distance to the nearest sampling or drilling

* Corresponding author: *Tel./Fax: +51989747200, E-mail address:* mcotrinat@unitru.edu.pe (M. A. C.-Teatino).

point, (vi) the average distance to the samples used in the estimation, and (vii) the number of drillholes utilized. Meanwhile, Owusu [27] highlights that geometric methods consider the quantity, proximity, and location of the data as key criteria for block estimation, including: (i) ellipsoidal search dimensions, (ii) number of drillholes, (iii) minimum distance to the nearest drillhole, (iv) average drillhole spacing, and (v) octant search declustering. Other approaches have also been used, such as drillhole spacing and density [28], Delaunay triangulation [29], and spacing calculation for both vertical and non-vertical drillholes [30]. Regarding geostatistical methods, several studies have proposed specific criteria for resource classification. Emery et al. [31] use variables, such as (i) kriging variance, (ii) conditional variance, (iii) relative kriging variance, and (iv) relative conditional variance. Mucha et al. [32] emphasize the use of the variogram as the primary source of parameters, whereas Taghvaeenezhad et al. [33] prioritize (i) estimation variance by kriging, (ii) kriging efficiency, and (iii) regression slope. Alternatively, Nowak et al. [34] propose an approach based on the indicator variogram [35, 36], where drilling data are transformed into binary values with a specific threshold, allowing continuity modelling as a basis for classification. Other methodologies include combining indicator kriging with standardized kriging variance to define a risk index [37], truncated Gaussian simulation applied to categorical variables such as rock type and mineralization [38], and conditional simulation of ore grades [39, 40]. Additionally, Silva et al. [41] introduced the use of cross-validation variance and classification in moving windows based on conditional simulation. Other strategies include the Resource Classification Index [42], which integrates combined variance, block estimation value, and a calibration factor, as well as error analysis in estimation relative to confidence intervals and production rates [43]. Previous studies have shown that uncertainty in resource estimation depends on model scale, with lower uncertainty in larger volumes due to the attenuation of extreme values [24, 39, 40, 44, 45]. In practice, these geometric and geostatistical criteria are applied through the manual definition of thresholds, even when they are combined in parallel [46–50].

Despite the wide range of available approaches, international codes do not establish a specific methodology for mineral resource classification. Instead, they recommend that the QP quantify the confidence level in the estimation before assigning a category, when necessary [9]. The absence of categorical guidelines reflects the inherent complexity of classification, as it is not feasible to define a single method applicable to all mineralization types and geological contexts [13]. Consequently, the final decision rests on the QP's judgment, who must select the most appropriate criteria for each specific case [25, 27]. Since different criteria can lead to significant variations in ore grade, metal content, and tonnage within each category, it is critical to evaluate their impact on resource estimation [46].

The literature has proposed various approaches for classifying mineral resources based on uncertainty. Some authors suggest the use of geostatistical simulations to assess the probability of resource occurrence [24, 39] or the application of multi-Gaussian kriging as an alternative to improve estimation accuracy [51]. However, other researchers argue that purely probabilistic approaches can be highly sensitive to parameter selection and, therefore, prone to errors. In this regard, it has been recommended that these methods be used as complementary tools alongside classification methodologies based on geometric and geological criteria, which are considered more transparent and replicable in mining practice [22]. In general, the classification of mineral resources serves as a key mechanism for reporting uncertainty in the mining industry. The classification into measured, indicated, and inferred resources provides a structured framework to communicate the confidence level in resource estimation [25, 52, 53]. Other uncertainty assessment strategies include kriging-based approaches [54, 55], probabilistic methods [56–58], geostatistical simulation [43, 44], and machine learning (ML) techniques [59, 60]. A widely adopted criterion in resource classification is the 15% rule, which stipulates that the estimated grade, metal content, and tonnage should exhibit a maximum error of 15% within a 90% confidence interval [61, 62].

Several studies have identified inconsistencies in the application of traditional numerical criteria for resource classification, both in geometric and geostatistical approaches, particularly when parameters are assigned block-by-block. Stephenson et al. [63] pointed out that this method can produce spatially inconsistent results that do not respect the geological continuity of the deposit, thus requiring additional post-processing smoothing. To address this issue, various strategies have been proposed, such as manual interpretation or the use of smoothing algorithms based on moving window statistics [50]. In this context, machine learning (ML) has emerged as a promising tool to enhance the classification of mineral resources. Cevik et al. [25] implemented an ML-based approach using a support vector machine (SVM) model with a radial basis function kernel, trained with spatial coordinates to reclassify blocks. Hernández [46] applied a similar methodology but utilized a multilayer artificial neural network (ANN). Additionally, Rossi et al. [55] recommended verifying global tonnage-grade curves before and after smoothing to assess the impact of processing on estimation accuracy. Previous studies have explored various ML techniques in resource estimation, highlighting the use of ANN, random forests (RF), SVM, and neuro-fuzzy models as the most frequently employed methods [64]. Furthermore, these approaches have demonstrated their ability to quantify resource uncertainty through confidence intervals in estimations [60, 62, 65]. Recent investigations have applied supervised machine learning algorithms to predict undiscovered mineral resources using techniques such as adaptive boosting (AdaBoost), gradient boosting decision trees (GBDT), and extreme gradient boosting (XGBoost) [66, 67]. In addition, recent studies have demonstrated the potential of ensemble and hybrid machine learning models to improve geological prediction tasks in mineral exploration. Farhadi et al. [68] introduced an ensemble approach based on the StackingC model, which outperformed traditional classifiers in lithological mapping by capturing complex nonlinear relationships in geochemical datasets. Similarly, Farhadi et al. [69] proposed a hybrid methodology combining machine learning regressors with concentration area fractal modeling to detect Pb-Zn anomalies in sediment-hosted deposits. In the Peruvian context, Cotrina et al. [70] compared supervised learning techniques including XGBoost, Random Forest, and deep neural networks for mineral resource categorization, demonstrating the accuracy and robustness of these models in geologically complex deposits.

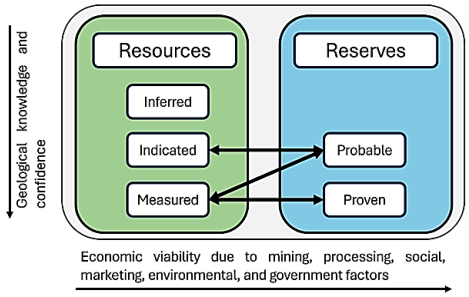

Figure 1. General relationship between mineral resources and reserves.

Despite advances in the application of machine learning for mineral resource estimation and classification, the selection of optimizers in neural network models remains an underexplored topic in this field. Existing literature has addressed the comparison of optimizers in other contexts, such as meteorological variable prediction [71] and image processing in computer vision [72], but their impact on mineral resource classification has not been extensively studied. Nanni et al. [73] analyzed the variants of the Adam optimizer based on the difference between the present and past gradients, demonstrating that the step size is optimally adjusted for each parameter. However, the influence of different optimizers on estimation accuracy, block smoothing, and uncertainty reduction in mineral resource classification remains an open research question.

In this context, the present study proposes an innovative methodology that addresses this knowledge gap through the following contributions:

- Mixed-variable block-by-block clustering using the k-prototypes

algorithm [74], an unsupervised machine learning method that simultaneously handles quantitative and qualitative data without any restrictions on the number of input features.

- Block smoothing using a multilayer artificial neural network, implementing different optimizers to mitigate the "spotted dog" effect inherent in block-by-block classification.
- Comparison of the impact of different optimizers on mineral resource classification, evaluating model accuracy, tonnage, and fine content. The optimizers Adam, RMSprop, SGD, and Adagrad are considered, providing a comparative analysis to determine which optimizer offers the best performance in this specific application.

This study is structured into four sections. Section 2 details the methodology used in the research, including the models and evaluation criteria. Section 3 presents the obtained results and discusses their relevance in comparison with previous studies. Finally, Section 4 outlines the study's conclusions, highlighting the implications of the findings and potential future research directions.

2. Materials and methods

This study proposes an integrated methodology for the classification of mineral resources in a copper deposit in Peru, combining geostatistical techniques with machine learning approaches. A multilayer artificial neural network (Multilayer Perceptron, MLP) is employed to smooth the block classification, utilizing different optimizers (Adam, RMSprop, SGD, and Adagrad). All models were trained in Python 3.11.7 within the Jupyter Notebook environment. The general workflow of the methodology is illustrated in Figure 2.

2.1. Geological setting

The copper deposit analyzed in this study is situated in the central Andes of Peru, at an approximate elevation of 4,600 meters above sea level. The regional geology comprises a complex lithological assemblage indicative of a porphyry-skarn metallogenic environment. The deposit is hosted in five distinct lithological units: magnetite skarn, granodiorite, dacite porphyry, calcareous sediments, and a volcanic unit locally referred to as the Catalina Formation. Copper and molybdenum mineralization is spatially distributed across all lithologies, though higher concentrations are typically found within the magnetite skarn (rock type 1) and granodiorite (rock type 2), suggesting a strong lithological control. Mineralization occurs predominantly as disseminated sulfides, veinlets, and hydrothermal breccia fillings, with alteration halos characteristic of porphyry systems. The deposit's structural framework, comprising faults and fracture systems, further influences the spatial continuity and grade variability of the ore body.

2.2. Data preparation

The database used in this study originates from a copper deposit in Peru, characterized by complex mineralization and significant geological heterogeneity. The study area is predominantly composed of magnetite skarn, granodiorite, dacite porphyries, calcareous sediments, and volcanic units. Due to confidentiality agreements, the name of the deposit and any additional information that could reveal its location or the identity of the mining company are not disclosed. The database consists of 185 diamond drill holes, with an average spacing of 30 meters and an average depth of approximately 480 meters. Mineralization is distributed across five lithologies, categorized as follows: rock 1 is magnetite skarn, rock 2 is granodiorite, rock 3 is dacite porphyry, rock 4 is calcareous sediments, and rock 5 is Catalina volcanic unit. To standardize the data and ensure consistency in subsequent analyses, drill hole samples were composited based on lithology, resulting in a total of 5,654 composites (see Figure 3).

The statistical analysis of the database determined that the average copper grade is 0.43%, with a variance of 0.084 and a standard deviation of 0.29. These values indicate low dispersion relative to the mean, suggesting a certain level of homogeneity in the copper grade distribution within the deposit. Table 1 presents the descriptive statistics of the database used in this study.

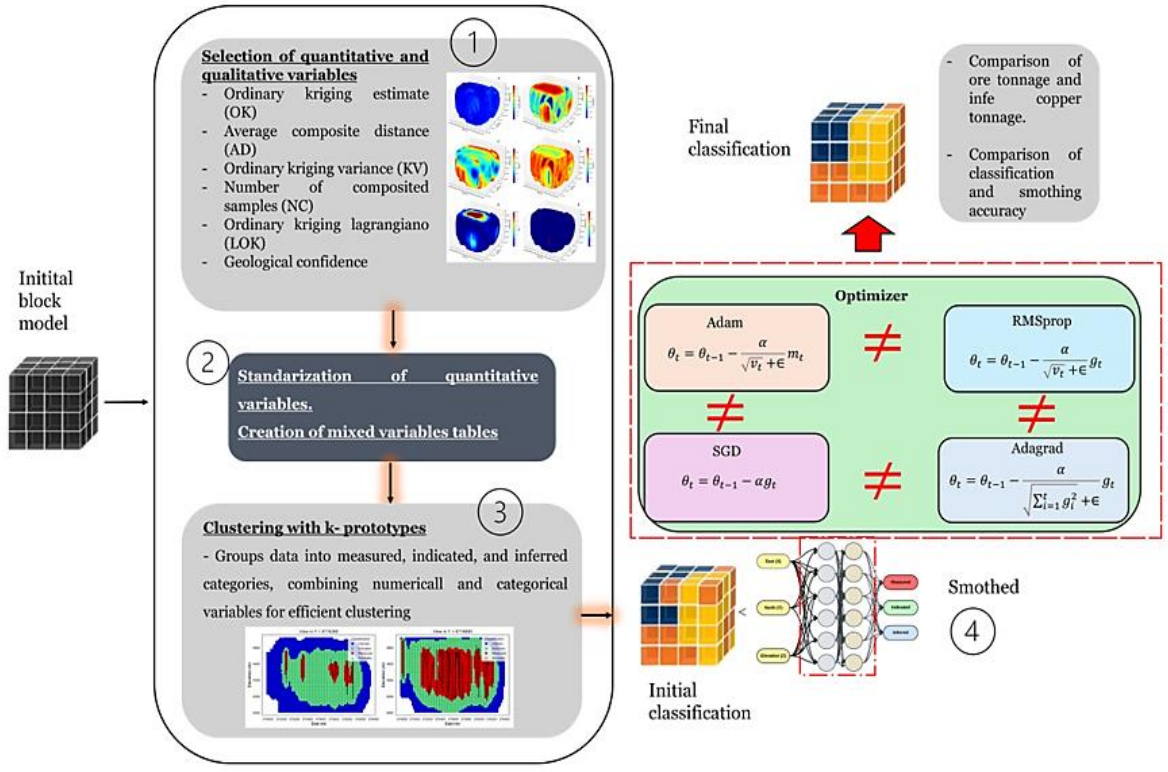

Figure 2. Research methodology flowchart.

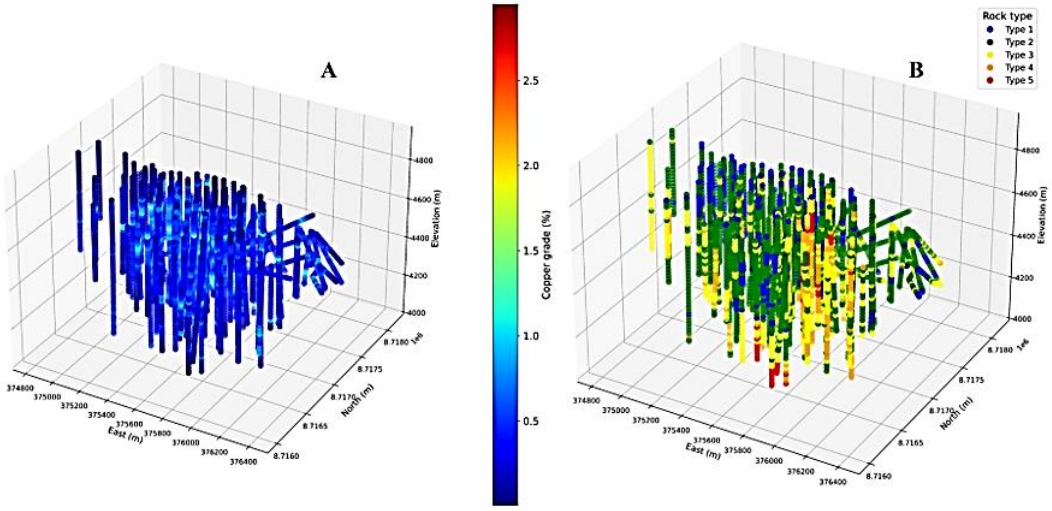

Figure 3. Drill hole distribution. A: copper grades. B: rock types.

Table 1. Descriptive statistics of the database.

Feature	East (m)	North (m)	Elevation (m)	Copper grade (%)	Molybdenum grade (%)	Rock type
Count	5654.00	5654.00	5654.00	5654.00	5654.00	5654
Mean	375606.25	8717015.68	4473.54	0.43	0.01	2.16
Std dev	307.24	393.54	169.54	0.29	0.01	0.78
Minimum	374821.06	8716003.08	4050.35	0.00	0.00	1.00
25%	375393.42	8716738.40	4340.07	0.23	0.00	2.00
50%	375602.29	8716995.80	4462.81	0.38	0.01	2.00
75%	375824.99	8717271.73	4607.49	0.58	0.02	3.00
Maximum	376414.81	8718153.15	4902.14	2.95	0.09	5.00
Variance	94394.00	154875.00	28743.00	0.084	0.0002	0.61

The grade distribution analysis reveals a positive skewness in both copper and molybdenum grades, indicating the presence of outliers and potential heterogeneity in the mineralization. Specifically, the copper grade ranges from a minimum (Y_{min}) of 0.002% to a maximum (Y_{max}) of 2.95%, with a mean of 0.43%. Similarly, the molybdenum grade varies between 0.00% and 0.09%, with an average of 0.01%. The histograms in Figure 4 highlight zones with high concentrations, contrasted with areas of low mineralization, emphasizing the geological variability of the deposit.

2.3. Selection of variables for classification

To estimate mineral resources, Ordinary Kriging (OK) was applied using SGEMS software [75, 76], with a block size of 20 x 20 x 20 meters. The estimation considered directional variograms of copper grade in three principal directions (0°, 45°, and 90°), reaching a sill value between 150 and 200 meters. A spherical variogram was used, with a maximum range of 250 meters, an intermediate range of 130 meters, and a minimum range of 115 meters. To ensure an adequate spatial representation of mineralization, a search ellipsoid was defined with a maximum range of 450 meters, a medium range of 250 meters, and a minimum range of 200 meters, resulting in the estimation of a total of 318443 blocks. Based on this estimation, six key variables were selected for the classification of mineral resources:

1. Ordinary kriging estimated grade (OK)
2. Average sample distance (AD)
3. Kriging variance (VOK)
4. Number of samples used in the estimation (NS)
5. Geological confidence (CG)
6. Ordinary kriging Lagrangian (LOK)

Each of these variables provides essential information for classifying mineral resources based on uncertainty and geological continuity.

Ordinary Kriging estimated grade (OK): The estimated mineral grade (Z^*) represents the interpolated concentration of copper in each block of the model, based on an optimal weighting of drilling data [77]. Ordinary Kriging minimizes the estimation error variance, producing optimal values for each block under the assumption of local stationarity [78, 79]. The estimation is defined as:

$$Z^*(x) = \sum_{i=1}^{n} \lambda_i Z(x_i) \quad (1)$$

Where: $Z^*(x)$ is the estimated grade at location x; $Z(x_i)$ is the measured grade at sample i, λ_i are the weights assigned by the Kriging system and n is the number of samples used in the estimation. This variable allows for differentiating zones of high and low mineral concentration, making it crucial in mineral resource classification.

Average sample distance (AD): represents the mean distance between the estimated block and the samples used in interpolation [80]. It is calculated as:

$$AD = \frac{1}{n}\sum_{i=1}^{n} d_i \quad (2)$$

Where: d_i is the distance between the block and sample i; n is the total number of samples used in the estimation. Blocks with higher AD values exhibit greater uncertainty in estimation, reflecting areas with lower drilling data density.

Kriging variance (VOK) (σ_k^2) quantifies the uncertainty associated with the estimation of each block. This variable plays a key role in mineral resource classification, as it provides a measure of confidence in the estimation [31, 41]. It is defined as:

$$\sigma_k^2 = \sum_{i=1}^{n} \lambda_i \gamma(x, x_i) \quad (3)$$

Where: $\gamma(x, x_i)$ is the variogram value for the distance between block location x and sample x_i. A high VOK value indicates greater uncertainty, suggesting that the interpolation is influenced by distant or scarce data.

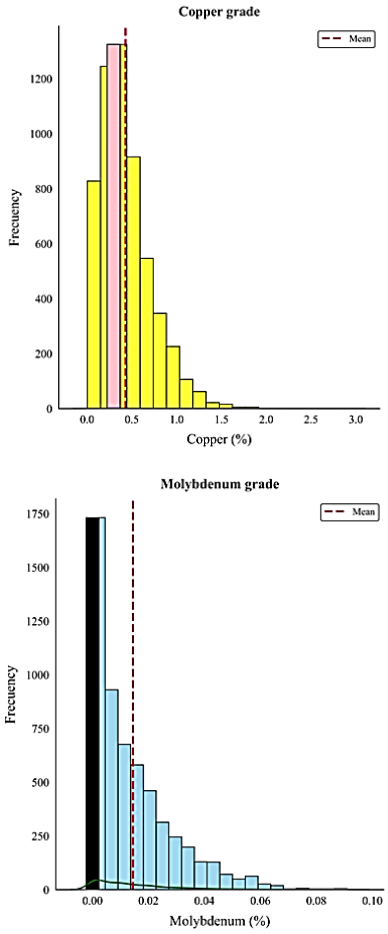

Figure 4. Grade distribution histograms. Up: copper grade. Down: Molybdenum grade.

Number of samples used in the estimation (NS): represents the total count of drilling data used in the estimation of each block [81]. It is expressed as:

$$NS = \sum_{i=1}^{n} 1 \quad (4)$$

A higher NS value implies greater confidence in the estimation, whereas low NS values indicate data-sparse zones, leading to higher uncertainty.

Geological confidence (CG): This index integrates information on spatial continuity and data quality [82]. It is calculated as:

$$\sum_{i=1}^{n} \lambda_i = 1 + \mu \quad (5)$$

Where μ is the Lagrange parameter. Higher μ values may indicate regions of high geological variability, whereas lower values suggest greater stability in interpolation.

Table 2 presents the statistical summary of the key variables utilized in the mineral resource classification process. The average estimated grade (OK) is 0.34%, while the kriging variance (KV) is 0.07. The average sample distance (AD) is 231.91 m, and the number of samples (NS) used in the estimation has a mean value of 124. Additionally, the geological confidence (CG) is 0.15, indicating the variability in estimation confidence. A 3D graphical representation of these variables is presented in Figure 5.

2.4. Multivariable mixed clustering using K-Prototypes

The classification of mineral resources requires the segmentation of blocks based on multiple variables, including both numerical and categorical characteristics. To address this issue, a multivariable mixed clustering model based on the K-Prototypes algorithm [74] was implemented. This method allows the simultaneous handling of continuous and discrete data, making it well-suited for mineral resource classification. A clustering scheme with three clusters (k=3) was established, determined by the data structure and the geological coherence of the deposit. To improve model convergence, the Huang initialization method was used, a widely validated approach in clustering problems involving mixed data types. The K-Prototypes algorithm extends the logic of K-Means [83] and K-Modes [84], enabling the segmentation of databases that contain both numerical and categorical variables. Given a mixed database X, consisting of a subset of numerical variables X_n and a subset of categorical variables X_c, the objective of the model is to minimize the following cost function:

$$J = \sum_{i=1}^{n} \sum_{j=1}^{k} \delta(x_i, c_j) \quad (6)$$

Where x_i represents an observation in the database and c_j e is the centroid of the assigned cluster.

The total distance between a given sample x_i and its assigned cluster centroid c_j is composed of two terms:

$$d(x_i, c_j) = d_n(x_i, c_j) + \gamma d_c(x_i, c_j) \quad (7)$$

Where $d_n(x_i, c_j)$ represents the Euclidean distance between the numerical variables and $d_c(x_i, c_j)$ measures the dissimilarity between categorical variables. For numerical variables, the distance is computed as the squared Euclidean norm between the observation and the centroid of the cluster:

$$d_n(x_i, c_j) = \|x_i - c_j\|^2 \quad (8)$$

For categorical variables, the matching distance is used, which counts the number of attributes that differ between an observation and its assigned cluster:

$$d_c(x_i, c_j) = \sum_{l=1}^{m} I(x_{il} \neq c_{jl}) \quad (9)$$

Where $I(x_{il} \neq c_{jl})$ is an indicator function that takes a value of 1 if the categorical attributes are different and 0 otherwise. The γ parameter in the equation regulates the influence of categorical variables in the clustering process. A higher γ value increases the importance of categorical dissimilarity, while lower values prioritize Euclidean distance for numerical features, allowing a more balanced segmentation based on both data types.

The K-Prototypes model was implemented using the kmodes library [84], which allows clustering techniques to be applied to mixed data types. Parallel processing was enabled with four execution cores ($n_{jobs} = 4$), optimizing the calculation speed and improving cluster assignment efficiency. To ensure result reproducibility, a random state of 17,276,365 was set. The full hyperparameter configuration of the K-Prototypes clustering model is detailed in Table 3.

Table 2. Statistical summary of variables used for mineral resource classification.

Feature	OK	AD	VOK	NS	LKO	CG
Count	318,443.0	318,443.0	318,443.0	318,443.0	318,443.0	318,443.0
Mean	0.34	231.91	0.07	124	-0.01	0.15
Std dev	0.15	59.19	0.03	70	0.01	0.36
Minimum	0.00	114.27	0.00	10	-0.06	0.00
25%	0.26	189.35	0.05	54	-0.01	0.00
50%	0.33	224.66	0.08	131	-0.00	0.00
75%	0.42	269.69	0.09	200	-0.00	0.00
Maximum	2.21	433.19	0.15	200	0.00	1.00

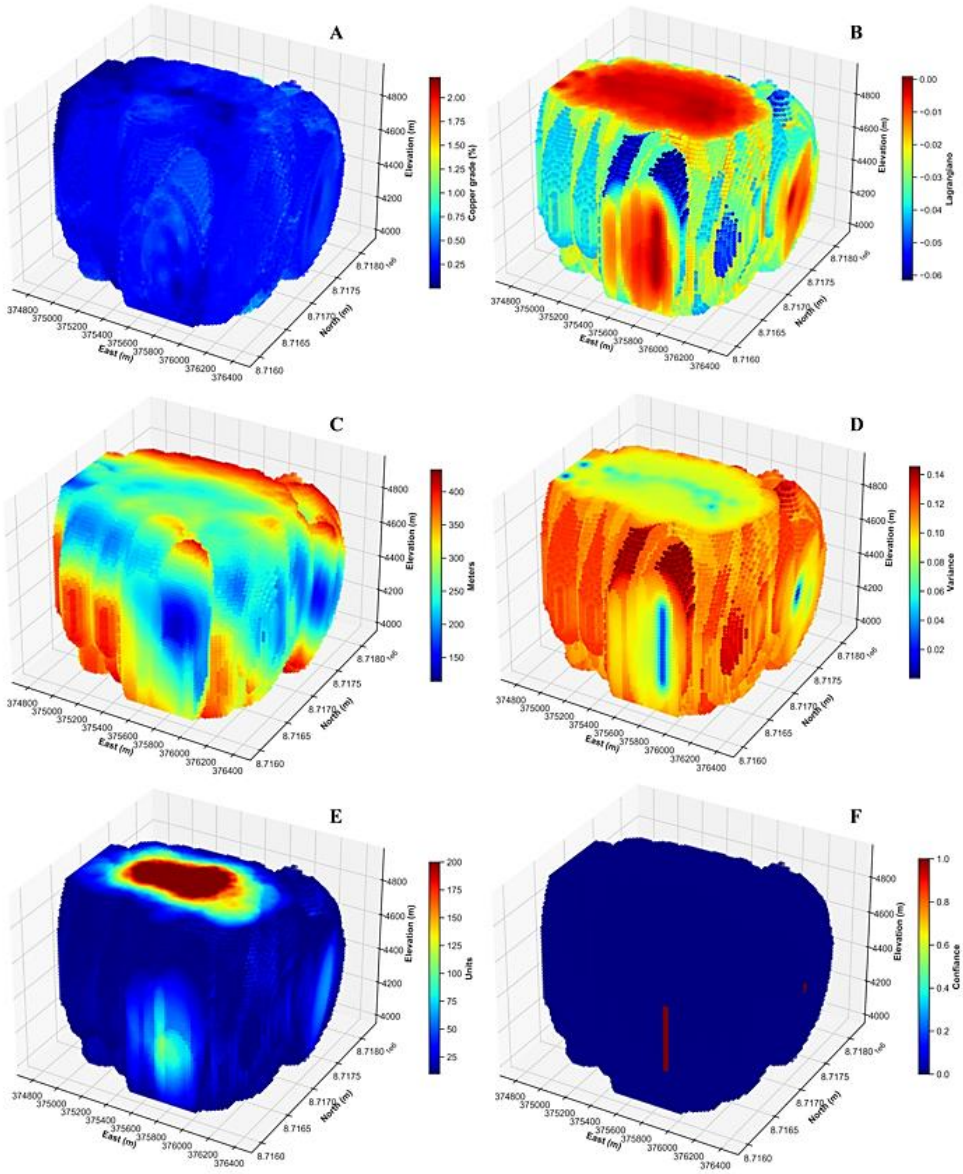

Figure 5. Key variables for mineral resource classification. A: Block model with ordinary kriging estimation. B: Ordinary kriging Lagrangian. C: Average composite distance. D: Ordinary kriging variance. E: Number of composites. F: Geological confidence.

Table 3. Hyperparameters of the K-Prototypes clustering model.

Model	Description	Value
K-Prototypes	n_clusters	3
	init	"Huang"
	n_jobs	4
	random_state	17,276,365
	categorical	[3]

2.5. Block smoothing using an artificial neural network

The block smoothing process was conducted using a Multilayer Perceptron Artificial Neural Network (MLP-ANN) [85–87] to mitigate the spatial variability introduced by block-by-block classification and enhance the geological coherence in the mineral resource classification. The neural network was implemented using the TensorFlow/Keras library [88], which facilitated model optimization.

The implemented MLP model consists of a two-layer architecture with 64 and 32 neurons, respectively, followed by an output layer responsible for generating the smoothed block classification. The ReLU (Rectified Linear Unit) activation function was selected for the hidden layers due to its ability to accelerate training convergence and mitigate the vanishing gradient problem. The ReLU function is defined as follows:

$$f(x) = \max(0, x) \tag{10}$$

Where x represents the neuron's pre-activation output. This function truncates negative values to zero, while positive values remain unchanged. Each layer in the neural network is mathematically modeled using the following equation:

$$h^{(l)} = f(W^{(l)} h^{(l-1)} + b^{(l)}) \tag{11}$$

Where $h^{(l)}$ represents the output of layer l, $W^{(l)}$ is the synaptic weight matrix, $b^{(l)}$ is the bias term, and $f(.)$ is the element-wise activation function. To prevent overfitting, a 10% dropout was incorporated. The hyperparameter configurations for the implemented MLP-ANN models are detailed in Table 4. As shown in Figure 6, the model was trained under four different configurations, each using a different optimizer to evaluate its accuracy in mineral resource

Table 4. Hyperparameters of the ANN configuration.

Model	Description	Conf. 1	Conf. 2	Conf. 3	Conf. 4
Multilayer perceptron (ANNs-MLP)	Hidden layers	2	2	2	2
	Neurons per layer	64, 32	64, 32	64, 32	64, 32
	Activation function	ReLU	ReLU	ReLU	ReLU
	Optimizer	Adam	RMSprop	SGD	Adagrad
	Learning rate	0.001	0.001	0.001	0.001
	Batch size	32	32	32	32
	Epochs	50	50	50	50
	Dropout	0.1	0.1	0.1	0.1

classification. The graphical representation of the artificial neural network architecture is presented in Figure 6.

Adam (adaptive moment estimation): Adam is an optimization method that combines the first and second moment estimates of the gradient, allowing for adaptive parameter updates with independent learning rates [89]. The weight update process follows the equations:

$$m_t = \beta_1 m_{t-1} + (1-\beta_1) g_t \quad (12)$$

$$v_t = \beta_2 v_{t-1} + (1-\beta_2) g_t^2 \quad (13)$$

$$\theta_t = \theta_{t-1} - \frac{\alpha}{\sqrt{v_t}+\epsilon} m_t \quad (14)$$

Where m_t and v_t are the first and second moment estimates of the gradient, θ_t represents the updated weights, α is the learning rate, and β_1, β_2 are decay rates. The variable g_t represents the gradient at time step t, and the variable ϵ is a very small constant used to avoid division by zero during the optimization process.

RMSprop (root mean square propagation): This optimizer adjusts the magnitude of weight updates by normalizing the gradient using a moving average of squared gradients [90]. It is defined as:

$$\theta_t = \theta_{t-1} - \frac{\alpha}{\sqrt{v_t}+\epsilon} g_t \quad (15)$$

RMSprop improves the stability of optimization when dealing with data of high variability.

SGD (stochastic gradient descent): SGD is a classical gradient descent algorithm, which updates weights at every iteration based on the computed gradient. However, it is highly sensitive to the learning rate and can oscillate in complex optimization landscapes [91]. The update rule is:

$$\theta_t = \theta_{t-1} - \alpha g_t \quad (16)$$

Adagrad (Adaptive gradient algorithm): Adagrad modifies the learning rate for each parameter independently, adapting to the scale of past gradients. This allows better handling of sparse data without requiring manual learning rate tuning [92]. The weight update formula is:

$$\theta_t = \theta_{t-1} - \frac{\alpha}{\sqrt{\sum_{i=1}^{t} g_i^2}+\epsilon} g_t \quad (17)$$

In all configurations, the learning rate was set to 0.001, with a batch size of 32 and a total of 50 epochs, ensuring training stability.

The evaluation of the artificial neural network model was conducted using classification metrics, including precision, recall, F1-score, and accuracy. These metrics assess the model's performance in correctly classifying blocks within the defined categories. Precision measures the proportion of correctly categorized blocks within a class relative to all blocks classified in that category:

$$Precision = \frac{TP}{TP+FP} \quad (18)$$

Where TP represents the true positives and FP the false positives.

Recall evaluates the model's ability to correctly identify blocks belonging to a specific category. To obtain a balanced measure between precision and recall, the F1-score is used, which combines both metrics into a single expression. This metric is particularly useful when assessing model performance in scenarios where class distribution is imbalanced [93, 94]. Finally, accuracy measures the total proportion of correctly classified blocks over the total number of evaluated blocks.

$$Recall = \frac{TP}{TP+FN} \quad (19)$$

$$F1-score = 2x\frac{Precision\ x\ Recall}{Precision+Recall} \quad (20)$$

$$Accuracy = \frac{TP+TN}{TP+TN+FP+FN} \quad (21)$$

Where FN represents false negatives. A high recall value indicates that the neural network successfully classifies most blocks that genuinely belong to a given class. TN represents true negatives. This metric provides an overall assessment of the model's performance, though it may be less representative in cases where class distributions are highly imbalanced.

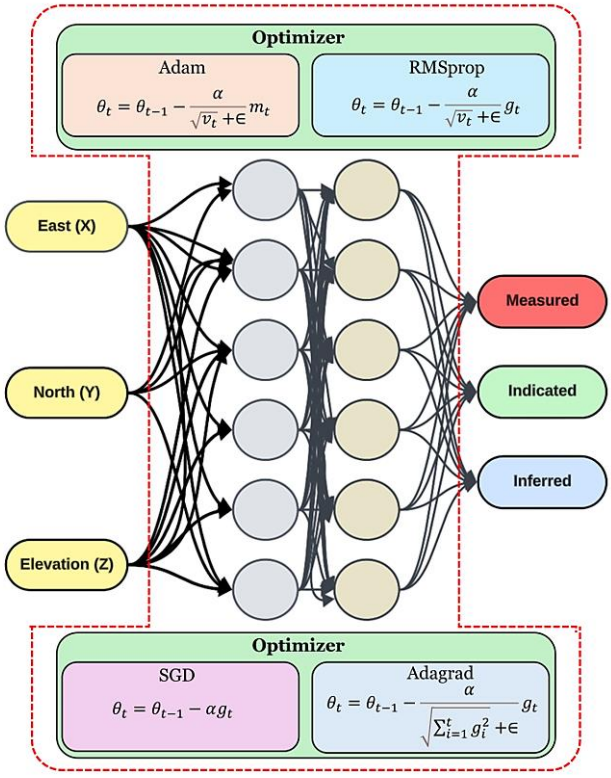

Figure 6. Architecture of the ANN with the optimizers used.

3. Results

3.1. Block by block mixed multivariable clustering using the k-prototypes algorithm

The classification of mineral resources was performed using the K-Prototypes algorithm applied to multiple 2D cross-sections of the block model. The results reveal three main categories, including Measured, Indicated, and Inferred each corresponding to varying degrees of geological confidence. As illustrated in Figure 7, the spatial distribution

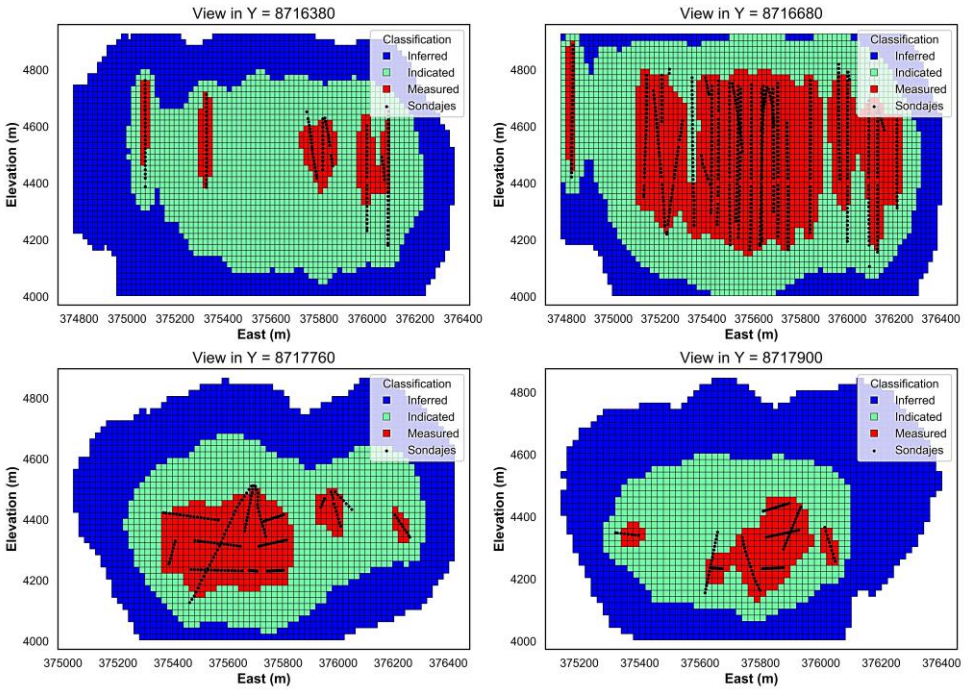

Figure 7. Classification of mineral resources using k-prototypes in different 2D sections.

of these classes demonstrates strong geological coherence: Measured resources (red) are tightly clustered around drill holes (black dots), Indicated resources (green) extend into areas with higher data density, and Inferred resources (blue) occupy the peripheries of the mineralized domain. The color gradients between classes reflect the enhanced spatial continuity and reduced fragmentation achieved through neural network smoothing.

This result is consistent with previous studies, which highlight that drill hole density and geological continuity are key factors in mineral resource classification [25, 27].

The clustering performance analysis, summarized in Table 5, indicates that the model achieves an adequate separation between clusters. The Silhouette Score of 0.3496 suggests an acceptable segmentation with some overlap between categories, while the Davies-Bouldin Index (0.9560) confirms a good separation between groups. Lastly, the Calinski-Harabasz Score (162,313) indicates a well-defined structure, with compact and well-separated clusters, supporting the effectiveness of the method in mineral resource classification. It is noted that some category overlap is expected due to the inherent variability in block classification [14].

Table 5. Clustering performance metrics using k-prototypes.

Metric	Value
Silhouette score	0.3496
Davies-Bouldin index	0.9560
Calinski-Harabasz Score	162,313

3.2. Block smoothing using a multilayer artificial neural network

To evaluate the effect of neural smoothing on resource estimation, the classification results obtained using the Adam optimizer were analyzed. This method provides a stable and precise adjustment of class boundaries, reducing abrupt transitions and improving spatial continuity across the model. As shown in Figure 8, the comparison before and after smoothing reveals a marked reduction in fragmentation, with more coherent transitions between Measured, Indicated, and Inferred categories. The Adam optimizer demonstrates an effective balance between convergence speed and classification stability, minimizing estimation noise without compromising accuracy.

The quantitative results, summarized in Table 6, indicate a precision score of 96% for Measured resources, 91% for Indicated resources, and 89% for Inferred resources, with an overall accuracy of 93%. The high F1-scores across all categories suggests that the model trained with Adam provides a reliable and geologically coherent classification. These findings are consistent with Desai [71], who demonstrated that Adam provides more stable convergence in machine learning applications due to its ability to dynamically adjust adaptive learning rates.

Table 6. Accuracy of the Adam optimizer in ANN for mineral resource classification.

Resources	Precision	Recall	F1-Score
Measured	0.96	0.97	0.97
Indicated	0.91	0.89	0.90
Inferred	0.89	0.91	0.90
Accuracy			0.93

The classification performance of the RMSprop optimizer was also assessed to analyze its behavior in the context of neural network smoothing. This method enhances the internal cohesion of classified blocks, although certain discontinuities remain evident at the boundaries between resource categories. As illustrated in Figure 9, the comparison between pre- and post-smoothing results shows improved consistency within classes, yet some segmentation persists likely due to RMSprop's sensitivity to data with high variability, as previously noted by Hassan et al. [72].

The results presented in Table 7indicate a precision of 96% for Measured resources, 92% for Indicated resources, and 87% for Inferred resources, with an overall accuracy of 92%.

Table 7. Accuracy of the RMSprop optimizer in ANN for mineral resource classification.

Resources	Precision	Recall	F1-Score
Measured	0.96	0.96	0.96
Indicated	0.92	0.86	0.89
Inferred	0.87	0.92	0.89
Accuracy			0.92

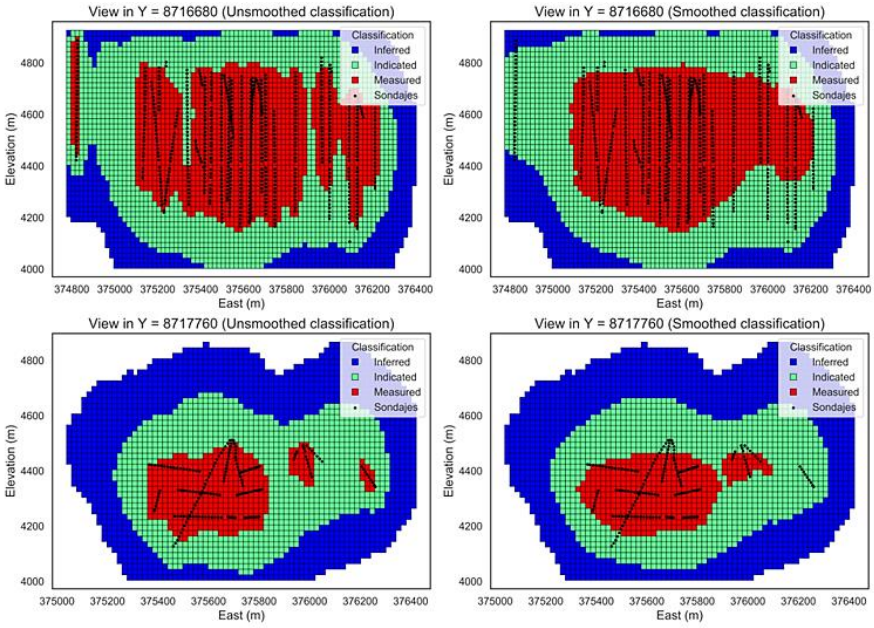

Figure 8. 2D visualization of mineral resource classification using the Adam optimizer in ANN. Left: classification without smoothing. Right: smoothed classification.

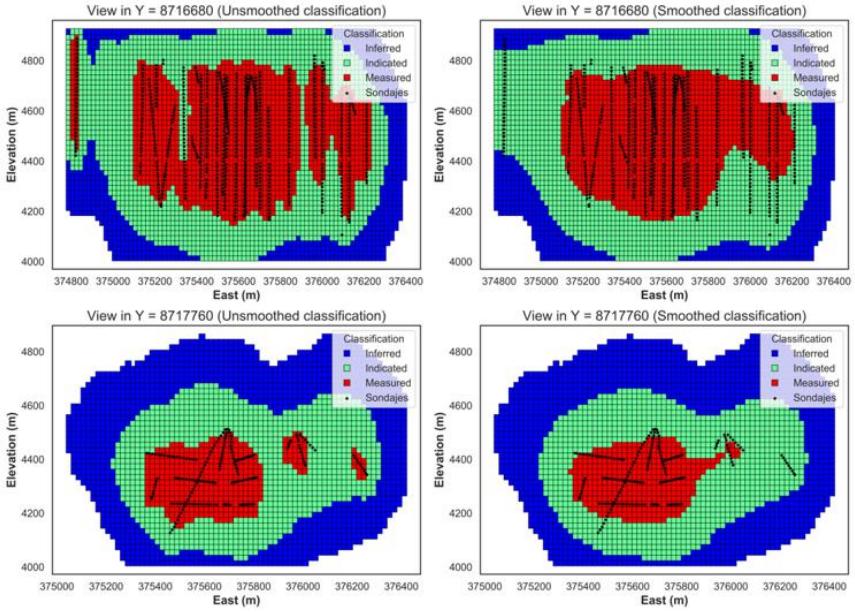

Figure 1. 2D visualization of mineral resource classification using the RMSprop optimizer in ANN. Left: classification without smoothing. Right: smoothed classification.

The application of the SGD optimizer to resource classification reveals limitations in smoothing performance, particularly in terms of spatial fragmentation. Compared to Adam and RMSprop, SGD exhibits slower convergence and greater sensitivity to hyperparameter settings. As evidenced in Figure 10, the resulting classification after smoothing shows higher levels of fragmentation, indicating that additional calibration is necessary to achieve coherent transitions between resource categories.

According to the results in Table 8, the precision reaches 96% for Measured resources, 91% for Indicated resources, and 89% for Inferred resources, with an overall accuracy of 92%. These findings align with those reported by Battalgazy et al. [14], who noted that the performance of SGD heavily depends on accurate hyperparameter calibration, particularly on the learning rate.

Figure 11 presents smoothing results using the Adagrad optimizer, highlighting its lower homogenization capability compared to other optimizers. Discontinuities are observed in the smoothed classification, particularly in the transition between Indicated and Inferred resource blocks, which may be attributed to Adagrad's adaptive learning rate strategy. While this strategy makes it suitable for sparse or highly heterogeneous data, in this case its limited ability to homogenize classified blocks exposes its constraints [22].

Table 8. Accuracy of the SGD optimizer in ANN for mineral resource classification.

Resources	Precision	Recall	F1-Score
Measured	0.96	0.96	0.96
Indicated	0.91	0.90	0.90
Inferred	0.89	0.90	0.90
Accuracy			0.92

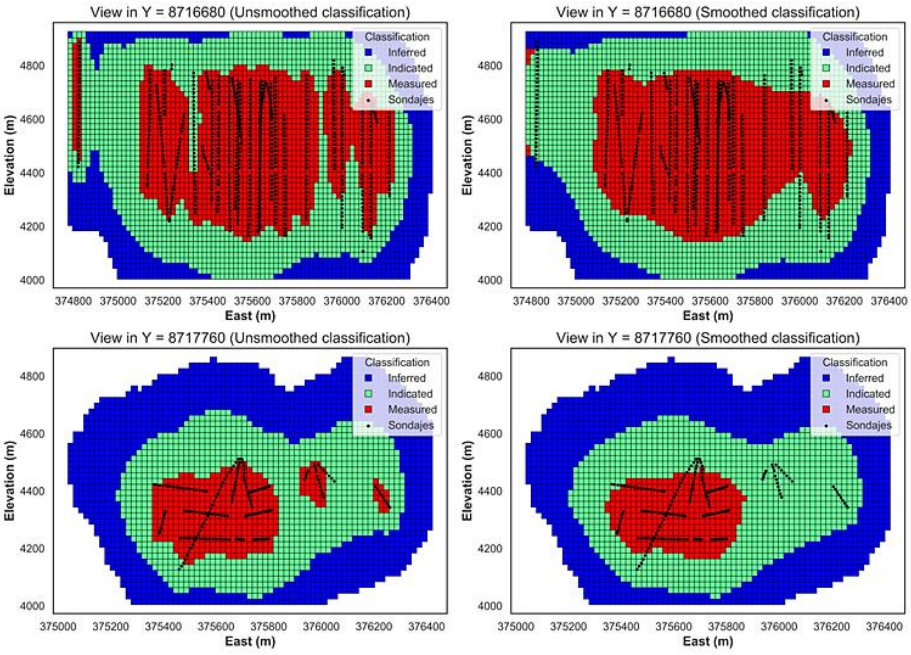

Figure 10. 2D visualization of mineral resource classification using the SGD optimizer in ANN. Left: classification without smoothing. Right: smoothed classification.

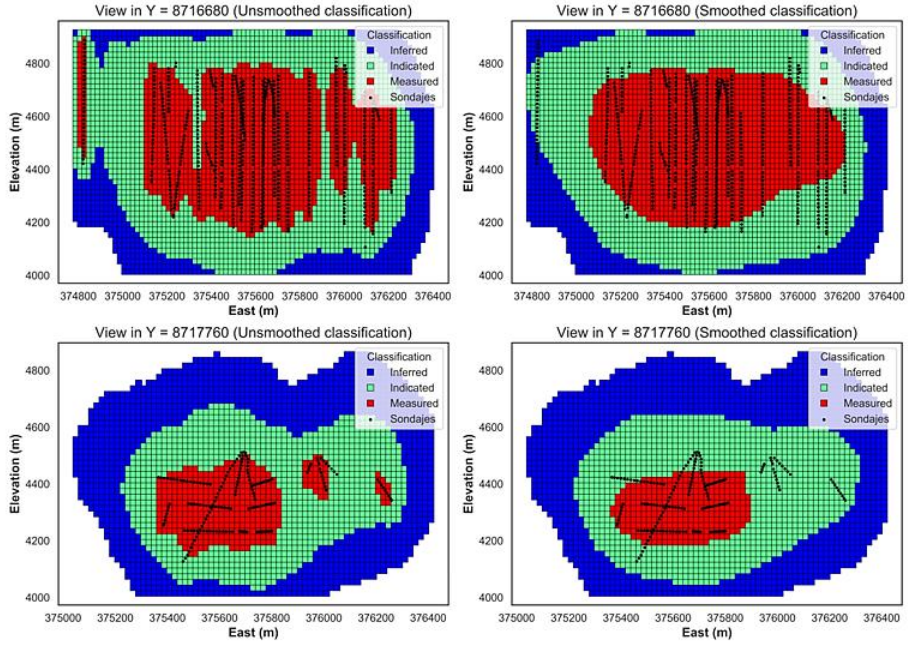

Figure 11. 2D visualization of mineral resource classification using the Adagrad optimizer in ANN. Left: classification without smoothing. Right: smoothed classification.

The values in Table 9 indicate a precision of 94% for Measured resources, 89% for Indicated resources, and 85% for Inferred resources, with an overall accuracy of 90%.

3.3. Optimizer comparison

Figure 12 presents the confusion matrices obtained for mineral resource classification using different optimizers in the artificial neural network (ANN). The Adam optimizer (A) exhibited the best classification distribution with the fewest prediction errors between categories, followed by RMSprop (B), which maintained high precision but showed slightly increased confusion between Indicated and Inferred resources. In contrast, SGD (C) and Adagrad (D) resulted in higher classification dispersion, indicating a lower generalization capacity of the model in these cases.

Table 11 quantifies the overall performance of each optimizer in terms of classification accuracy. The Adam optimizer achieved the highest accuracy (93%), followed by RMSprop and SGD (92%), while Adagrad obtained the lowest accuracy (90%), demonstrating its lower effectiveness in mineral resource classification. These findings align with studies emphasizing Adam's superiority in complex classification applications [71, 73]. Figure 13 compares 2D block classification results obtained through K-Prototypes clustering (A) before smoothing and after applying different ANN optimizers (B, C, D, and E for Adam, RMSprop, SGD, and Adagrad, respectively). It is evident that Adam and RMSprop produce a more coherent spatial distribution, while SGD and Adagrad result in greater spatial fragmentation, reflecting lower classification stability.

Table 10. Computational cost in mineral resource classification

Optimizer	Epochs completed	Time (seconds)
Adam	48/50	490
RMSprop	47/50	534
SGD	45/50	485
Adagrad	47/50	550

Table 11: Accuracy comparison in mineral resource classification.

Metric	Accuracy
ANN-Adam	0.93
ANN-RMSprop	0.92
ANN-SGD	0.92
ANN-Adagrad	0.90

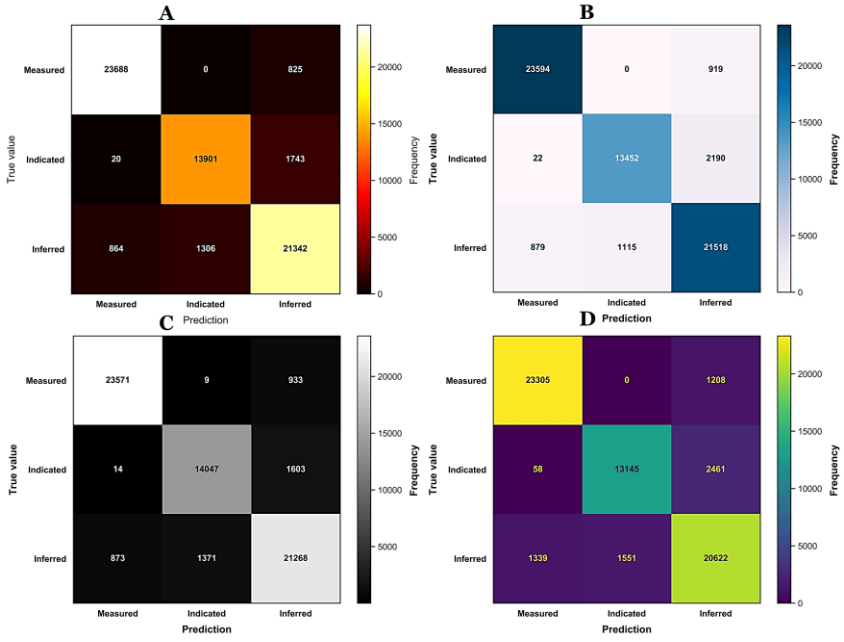

Figure 12. Confusion matrix for mineral resource classification using ANN. A: Adam optimizer. B: RMSprop optimizer. C: SGD optimizer. D: Adagrad optimizer.

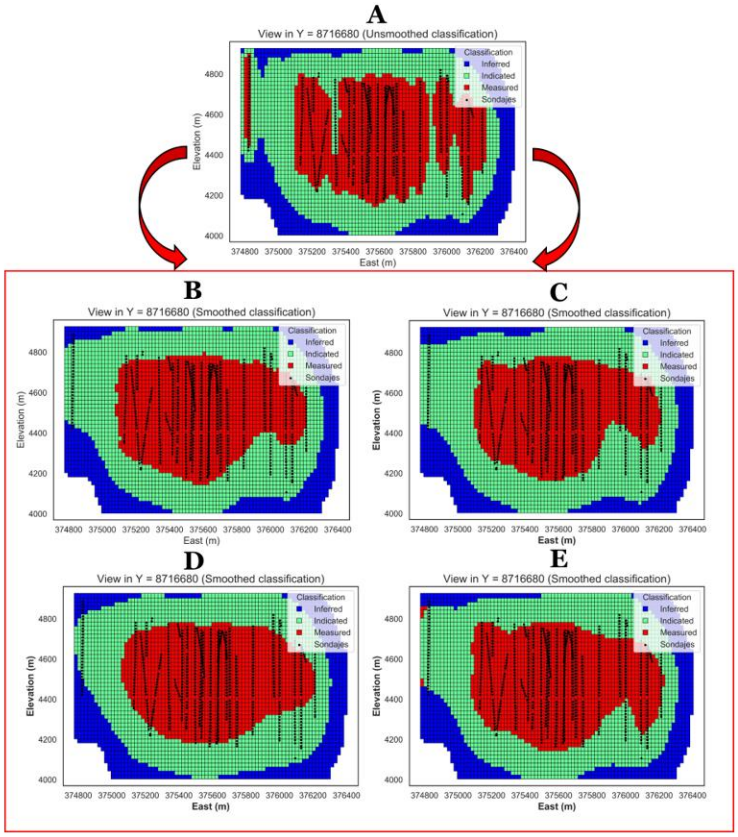

Figure 13. 2D visualization of mineral resource block classification. A: K-Prototypes classification without smoothing. B: Smoothed classification with Adam optimizer. C: Smoothed classification with RMSprop optimizer. D: Smoothed classification with SGD optimizer. E: Smoothed classification with Adagrad optimizer.

Figure 14 presents the box plots of the study variables for mineral resource classification using different optimizers. These visualizations illustrate the distribution and variability of key parameters across the Adam, RMSprop, SGD, and Adagrad optimizers.

Figures 15, 16, and 17 depict the tonnage vs. mean copper grade relationships for Measured, Indicated, and Inferred resources, respectively. In general, the Adam and RMSprop optimizers exhibit a more stable trend compared to SGD and Adagrad, indicating greater reliability in mineral resource estimation. A progressive decrease in mean grade is observed as tonnage increases, which is an expected trend in mineral resource classification. The classification of mineral resource blocks exhibits notable differences among the evaluated optimizers. The SGD optimizer produced the highest number of measured resource blocks (76,842 blocks), whereas RMSprop yielded the lowest (72,643 blocks). Conversely, in the indicated resource category, RMSprop classified the highest number of blocks (123,858), while SGD had the fewest (119,859). In the inferred resource category, the results were more consistent across all optimizers, ranging between 121,742 and 123,169 blocks, with Adagrad reporting the highest. These findings suggest that models trained with Adam and SGD tend to classify a larger number of measured blocks, likely due to their parameter adjustment and regularization capabilities. This aligns with Cevik et al. [25], who emphasized that model performance strongly depends on the optimizer's parameters and the density of available data (see Table 12).

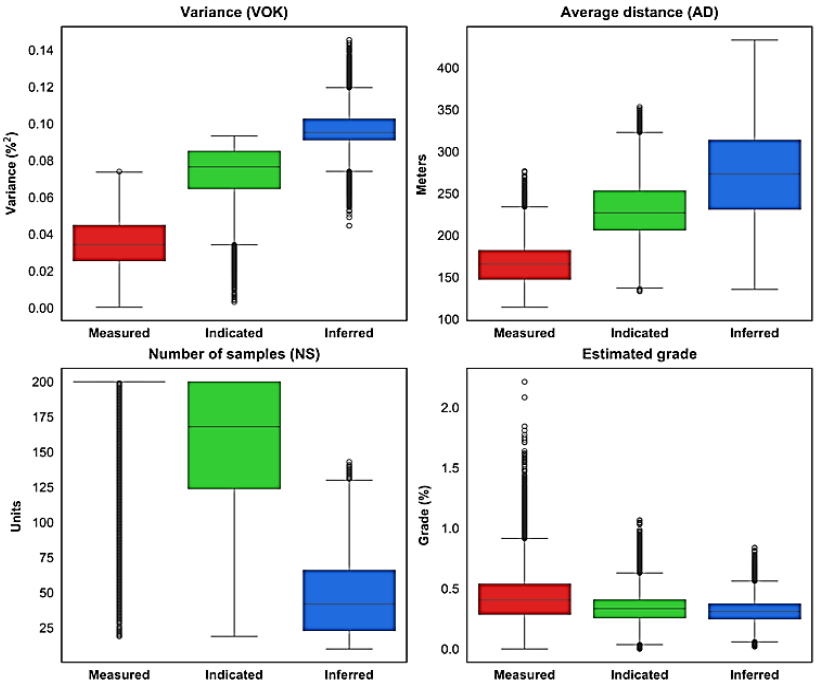

Figure 14. Box plot of study variables for mineral resource classification using different optimizers.

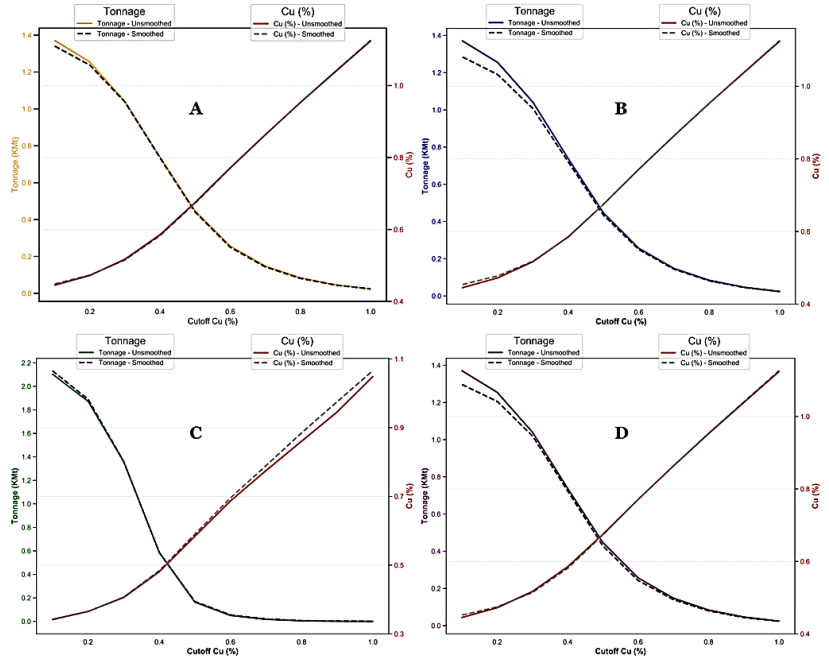

Figure 15. Tonnage–mean grade curves for measured resources. A: Adam. B: RMSprop. C: SGD. D: Adagrad.

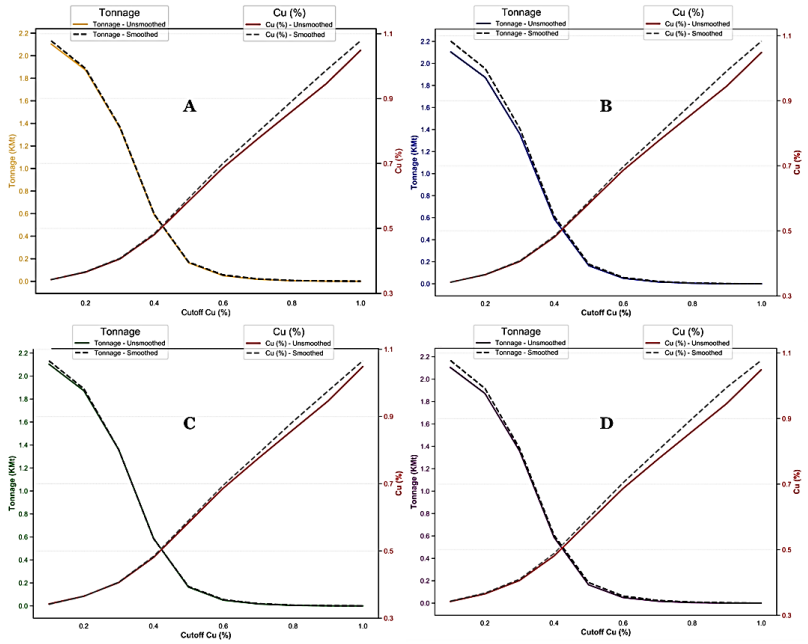

Figure 16. Tonnage–mean grade curves for indicated resources. A: Adam. B: RMSprop. C: SGD. D: Adagrad.

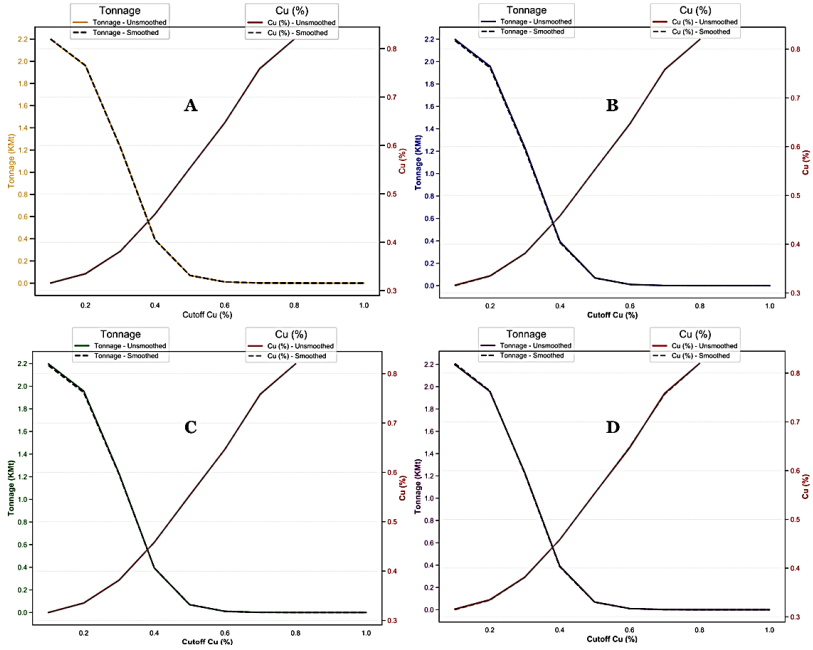

Figure 17. Tonnage–mean grade curves for inferred resources. A: Adam. B: RMSprop. C: SGD. D: Adagrad.

Table 12. Comparison of the number of blocks classified across mineral resource categories

Resource	ANN-Adam	ANN-RMSprop	ANN-SGD	ANN-ADAgrad
Measured	75,869.00	72,643.00	76,842.00	73,198.00
Indicated	120,039.00	123,858.00	119,859.00	122,076.00
Inferred	122,535.00	121,942.00	121,742.00	123,169.00

The total tonnage estimation also differs among optimizers. Models trained with Adam and SGD produced the highest tonnage values in the measured resource category, at 1,395.99 Mt and 1,413.89 Mt, respectively. Conversely, RMSprop and Adagrad reported lower values, at 1,336.63 Mt and 1,346.84 Mt, respectively. In the indicated resource category, RMSprop generated the highest total tonnage (2,278.99 Mt), while SGD produced the lowest (2,205.41 Mt). For inferred resources, the estimates were more homogeneous across optimizers, with differences of approximately 26 Mt, with Adagrad having the highest estimation (2,266.31 Mt) and SGD the lowest (2,240.05 Mt). These variations highlight the optimizer's influence on total tonnage estimation and resource classification (see Table 13). The fine copper tonnage analysis further underscores optimizer-specific variations. SGD and Adam yielded the highest estimates for measured resources, at 5.47 Mt and 5.40

Mt, respectively, whereas RMSprop and Adagrad recorded lower values, at 5.17 Mt and 5.33 Mt, respectively. In the indicated resource category, RMSprop (6.77 Mt) and Adagrad (6.67 Mt) achieved the highest fine copper estimates, while SGD and Adam provided similar values (6.55 Mt and 6.56 Mt, respectively). In the inferred resource category, the differences between optimizers were marginal, ranging from 6.25 Mt to 6.32 Mt, with Adagrad producing the highest estimate. These findings indicate that SGD and Adam tend to yield higher fine copper tonnage for measured resources, whereas RMSprop and Adagrad favor higher values for indicated and inferred resources (see Table 14).

These variations highlight the impact of optimizer selection on model stability and resource estimation accuracy [14, 46]. Furthermore, Adam and RMSprop exhibit more stable trends, aligning with the classification accuracy and consistency criteria established by Rossi et al. [55].

Table 13. Comparison of total tonnage across mineral resource categories.

Resource	ANN-Adam (Mt)	ANN-RMSprop (Mt)	ANN-SGD (Mt)	ANN-ADAgrad (Mt)
Measured	1395.99	1336.63	1413.89	1346.84
Indicated	2208.72	2278.99	2205.41	2246.20
Inferred	2254.64	2243.73	2240.05	2266.31

Table 14. Comparison of fine copper tonnage across mineral resource categories.

Resource	ANN-Adam (Mt)	ANN-RMSprop (Mt)	ANN-SGD (Mt)	ANN-ADAgrad (Mt)
Measured	5.40	5.17	5.47	5.33
Indicated	6.56	6.77	6.55	6.67
Inferred	6.29	6.26	6.25	6.32

4. Conclusions

The objective of this study was to evaluate the accuracy of different optimizers in mineral resource classification using a multilayer artificial neural network (MLP-ANN), with a particular focus on block smoothing and on reducing spatial fragmentation. The results demonstrated that the Adam optimizer achieved the highest overall accuracy, at 93%, outperforming RMSprop and SGD (92%) and Adagrad (90%). Additionally, Adam improved spatial continuity in the classification, particularly in measured resources, where it classified 75869 blocks with a total tonnage of 1395.99 Mt and a fine copper tonnage of 5.40 Mt. These findings highlight the effectiveness of Adam in complex geological applications, providing a more reliable and geologically consistent classification aligned with the characteristics of the deposit. The analysis of other optimizers revealed that RMSprop yielded a higher estimate for indicated resources, with a total tonnage of 2278.99 Mt and a fine copper tonnage of 6.77 Mt, while SGD exhibited strong performance in measured resources, reporting the highest fine copper tonnage (5.47 Mt). Adagrad, despite having the lowest overall accuracy, resulted in the highest estimation for inferred resources, classifying 123169 blocks with a total tonnage of 2266.31 Mt and a fine copper tonnage of 6.32 Mt. These variations emphasize how optimizer selection influences mineral resource estimation and classification, providing valuable insights for strategic mine planning.

Among the limitations of this study are the dependency on database characteristics, such as drill hole density and geological heterogeneity, which suggests the need to validate these results in other deposits under different conditions. An important identified limitation in the application of artificial neural networks is their high computational cost, especially which is relevant in contexts with hardware limitations or large-scale databases. Future research could explore dynamic hyperparameter optimization during model training, integrating hybrid approaches that combine neural networks with traditional geostatistical methods. Additionally, the implementation of advanced deep learning techniques, such as convolutional neural networks or attention-based models, could further enhance classification accuracy and model stability in mineral resource estimation.

References

[1] Coates, D. (1985). Mineral resources. In Geology and Society, 19–46.

[2] Dubiński, J. (2013). Sustainable Development of Mining Mineral Resources. Journal of Sustainable Mining, 12(1), 1-6. doi:https://doi.org/10.7424/jsm130102.

[3] Ericsson, M., Löf, O. (2019). Mining's contribution to national economies between 1996 and 2016. Mineral Economics, 32, 223-250. doi:https://doi.org/10.1007/s13563-019-00191-6.

[4] Van Gosen, B., Verplanck, P., Long, K., Gambogi, J., Seal, R. (2014). The Rare-Earth Elements: Vital to Modern Technologies and Lifestyles. US Geological Survey: Reston, VA, USA.

[5] Henckens, MLCM., Biermann, FHB., Driessen, PPJ. (2019). Mineral resources governance: A call for the establishment of an International Competence Center on Mineral Resources Management. Resour Conserv Recycl, 141, 255-263. doi:https://doi.org/10.1016/j.resconrec.2018.10.033.

[6] Crowson, PCF. (2011). Mineral reserves and future minerals availability. Mineral Economics, 24, 1-6. doi:https://doi.org/10.1007/s13563-011-0002-9.

[7] Zerzour, O., Gadri, L., Hadji, R., Mebrouk, F., Hamed, Y. (2021). Geostatistics-Based Method for Irregular Mineral Resource Estimation, in Ouenza Iron Mine, Northeastern Algeria. Geotechnical and Geological Engineering, 39, 3337-3346. doi:https://doi.org/10.1007/s10706-021-01695-1.

[8] Hartman, HL., Mutmansky, JM. (2002). Introductory mining engineering. Introductory Mining Engineering.

[9] CIM. (2019). Estimation of mineral resources & mineral reserves best practice guidelines. Canadian Institute of Mining.

[10] JORC Code. (2012). Australasian code for reporting of exploration results, mineral resources and ore reserves. AusIMM 44.

[11] SAMREC. (2016). The South African code for the reporting of exploration results, mineral resources and mineral reserves (the SAMREC Code. South African Mineral Resource Committee.

[12] Goodfellow, RC., Dimitrakopoulos, R. (2016). Global optimization of open pit mining complexes with uncertainty. Applied Soft Computing Journal, 40, 292-304. doi:https://doi.org/10.1016/j.asoc.2015.11.038.

[13] Menin, R., Diedrich, C., Reuwsaat, JD., De Paula, WF. (2017). Drilling Grid Analysis for Defining Open-Pit and Underground Mineral Resource Classification through Production Data. Geostatistics Valencia 2016, 271-285. doi:https://doi.org/10.1007/978-3-319-46819-8_18.

[14] Battalgazy, N., Madani, N. (2019). Categorization of mineral resources based on different geostatistical simulation algorithms: a case study from an iron ore deposit. Nat Resour Res, 28:1329–1351. doi:https://doi.org/10.1007/s11053-019-09474-9.

[15] Afzal, P., Gholami, H., Madani, N., Yasrebi, A., Sadeghi, B. (2023). Mineral Resource Classification Using Geostatistical and Fractal Simulation in the Masjed Daghi Cu–Mo Porphyry Deposit, NW Iran. Minerals, 13(3), 370. doi:https://doi.org/10.3390/min13030370.

[16] Guardiano, E., Parker, H., Isaaks, E. (1995). Prediction of Recoverable Reserves Using Conditional Simulation: A Case Study for the Fort Knox Gold Project, Alaska. Unpublished Technical Report; Mineral Resource Development Inc.: Port Moresby, Papua New Guinea.

[17] Kingston, G. (1977). Reserve classification of identified nonfuel mineral resources by the bureau of mines minerals availability system. Journal of the International Association for Mathematical Geology, 9, 273–279. doi:https://doi.org/10.1007/BF02272389.

[18] Dimitrakopoulos, R., Chou, C., Godoy, M. (2008). Resource / Reserve Classification with Integrated Geometric and Local Grade Variability Measures. Cosmo 08.

[19] Asghari, O., Esfahani, NM. (2014). Erratum to: A new approach for the geological risk evaluation of coal resources through a geostatistical simulation. Arabian Journal of Geosciences, 7, 839. doi:https://doi.org/10.1007/s12517-013-1262-1.

[20] Peattie, R., Dimitrakopoulos, R. (2013). Forecasting Recoverable Ore Reserves and Their Uncertainty at Morila Gold Deposit, Mali: An Efficient Simulation Approach and Future Grade Control Drilling. Math Geosci, 45, 1005-1020. doi:https://doi.org/10.1007/s11004-013-9478-x.

[21] Tajvidi, E., Monjezi, M., Asghari, O., Emery, X., Foroughi, S. (2015). Application of joint conditional simulation to uncertainty quantification and resource classification. Arabian Journal of Geosciences, 8, 455-463. doi:https://doi.org/10.1007/s12517-013-1133-9.

[22] Deustch, C., Leaungthong, O., Ortiz, J. (2007). Case for geometric criteria in resources and reserves classifcation. Trans Soc Min Metall Explor 322.

[23] Dominy, S., Stephenson, P., Annels, A. (2001). Classification and reporting of mineral resources for high-nugget effect gold vein deposits. Exploration and Mining Geology, 10, 215–233.

[24] Dohm, C. (2005). Quantifiable Mineral Resource Classification: A Logical Approach. Geostatistics Banff 2004, 333-342. doi:https://doi.org/10.1007/978-1-4020-3610-1_34.

[25] Cevik, IS., Leuangthong, O., Caté, A., Ortiz, JM. (2021). On the Use of Machine Learning for Mineral Resource Classification. Min Metall Explor, 38, 2055-2073. doi:https://doi.org/10.1007/s42461-021-00478-9.

[26] Stephenson, P., Stoker, P. (2001). Mineral resource and ore reserve estimation - the AusIMM guide to good practice (monograph 23). Miner Eng, 14(9). doi:https://doi.org/10.1016/s0892-6875(01)80033-9.

[27] Owusu, S. (2019). Critical Review of Mineral Resource Classification Techniques in the Gold Mining Industry. Insights in Mining Science & Technology, 1(3), 555564. doi:https://doi.org/10.19080/imst.2019.01.555564.

[28] Machuca-Mory, D., Deutsch, C. (2006). A Program for Robust Calculation of Drillhole Spacing in Three Dimensions.

[29] Delaunay, B. (1934). Sur la sphere vide. Bulletin de l'Académie des Sciences de l'URSS 6.

[30] Wilde, B., Deutsch, C V. (2010). Data spacing and uncertainty: Quantification and complications. IAMG 2010 Budapest - 14th Annual Conference of the International Association for Mathematical Geosciences.

[31] Emery, X., Ortiz, JM., Rodríguez, JJ. (2006). Quantifying uncertainty in mineral resources by use of classification schemes and conditional simulations. Math Geol, 38, 445-464. doi:https://doi.org/10.1007/s11004-005-9021-9.

[32] Mucha, J., Wasilewska-Błaszczyk, M., Augusčik, J. (2015). Categorization of mineral resources based upon geostatistical estimation of the continuity of changes of resource parameters. Proceedings of IAMG 2015 - 17th Annual Conference of the International Association for Mathematical Geosciences.

[33] Taghvaeenezhad, M., Shayestehfar, M., Moarefvand, P., Rezaei, A. (2020). Quantifying the criteria for classification of mineral resources and reserves through the estimation of block model uncertainty using geostatistical methods: a case study of Khoshoumi Uranium deposit in Yazd, Iran. Geosystem Engineering, 23(4), 216-225. doi:https://doi.org/10.1080/12269328.2020.1748524.

[34] Nowak, M., Leuangthong, O. (2019). Optimal drill hole spacing for resource classification. Mining Goes Digital - Proceedings of the 39th international symposium on Application of Computers and Operations Research in the Mineral Industry, APCOM 2019. doi:https://doi.org/10.1201/9780429320774-14.

[35] Journel, AG. (1983). Nonparametric estimation of spatial distributions. Journal of the International Association for Mathematical Geology, 15, 445-468. doi:https://doi.org/10.1007/BF01031292.

[36] Jelvez, E., Ortiz, J., Morales, N., Askari, H., Nelis, G. (2023). A Multi-Satage Methodology for Long-Term Open-Pit Mine Production Planning under Ore Grade Uncertainty. Mathematics, 11(18).

[37] Ribeiro, DT., Filho, CGM., de Souza, LE., Costa, JFCL., de Almeida D del PM. (2012). Utilização de critérios geoestatísticos para comparação de malha de sondagem visando à maximização da quantidade de recursos. Revista Escola de Minas, 65(1). doi:https://doi.org/10.1590/S0370-44672012000100016.

[38] Madani, N. (2020). Mineral resource classification based on uncertainty measures in geological domains. Springer Series in Geomechanics and Geoengineering, 157-164. doi:https://doi.org/10.1007/978-3-030-33954-8_19.

[39] Wawruch, TM., Betzhold, JF. (2005). Mineral Resource Classification Through Conditional Simulation. Geostatistics Banff 2004, 479-489. doi:https://doi.org/10.1007/978-1-4020-3610-1_48.

[40] Isatelle, F., Rivoirard, J. (2019). Mineral Resources classification of a nickel laterite deposit: Comparison between conditional simulations and specific areas. J South Afr Inst Min Metall, 119(10). doi:https://doi.org/10.17159/2411-9717/660/2019.

[41] Silva, DSF., Boisvert, JB. (2014). Mineral resource classification: A comparison of new and existing techniques. J South Afr Inst Min Metall 114.

[42] Arik, A. (2002). Comparison of resource classification methodologies with a new approach. 30th International Symposium on the Application of Computers and Operations Research in the Mineral Industry.

[43] Abzalov, M. (2016). Methodology of the mineral resource

classification. Modern Approaches in Solid Earth Sciences, 355-363. doi:https://doi.org/10.1007/978-3-319-39264-6_28.

[44] Caers, J. (2011). Modeling Uncertainty in the Earth Sciences. Modeling Uncertainty in the Earth Sciences. doi:https://doi.org/10.1002/9781119995920.

[45] Pyrcz, M., Deutsch, C. (2014). Geostatistical Reservoir Modeling (2nd Edition). Oxford University Press.

[46] Hernández, H. (2024). A semiautomatic multi criteria method for mineral resources classification. Applied Earth Science: Transactions of the Institutions of Mining and Metallurgy, 133, 211–223

[47] Zuo, M., Wang, T. (2021). Research on reserve classification of solid mineral resources in China and western countries. IOP Conf Ser Earth Environ Sci, 631. doi:https://doi.org/10.1088/1755-1315/631/1/012044.

[48] Duggan, S., Grills, A., Stiefenhofer, J., Thurston, M. (2017). Development of a best-practice mineral resource classification system for the de Beers group of companies. J South Afr Inst Min Metall, 117(12). doi:https://doi.org/10.17159/2411-9717/2017/v117n12a6.

[49] Mohanlal, K., Stevenson, P. (2010). Anglo American Platinum's approach to resource classification case study—Boschkoppie/Styldrift minewide UG2 project. The 4th International Platinum Conference, Platinum in Transition 'Boom or Bust.

[50] Rocha V, A., Bassani, MA. (2023). Practical application of a multi-layer scorecard workflow (MLSW) for comprehensive mineral resource classification. Applied Earth Science: Transactions of the Institute of Mining and Metallurgy. doi:https://doi.org/10.1080/25726838.2023.2244775.

[51] Ortiz, J., Deutsch, C. (2003). A practical way to summarize uncertainty for classifcation. Centre for computational geostatistics, report fve, University of Alberta 14.

[52] Glacken, I., Snowden, D. (2001). Mineral resource estimation, In Edwards, A. C.

[53] Revuelta, MB. (2018). Mineral Resources :From Exploration to Sustainability Assessment.

[54] Da Rocha, MM., Yamamoto, JK. (2000). Comparison between kriging variance and interpolation variance as uncertainty measurements in the Capanema iron mine, State of Minas Gerais-Brazil. Natural Resources Research, 9, 223-235. doi:https://doi.org/10.1023/a:1010195701968.

[55] Rossi, ME., Deutsch, C V. (2014). Mineral Resource Estimation. doi:https://doi.org/10.1007/978-1-4020-5717-5.

[56] Emery, X. (2008). Uncertainty modeling and spatial prediction by multi-Gaussian kriging: Accounting for an unknown mean value. Comput Geosci, 34(11), 1431-1442. doi:https://doi.org/10.1016/j.cageo.2007.12.011.

[57] McManus, S., Rahman, A., Horta, A., Coombes, J. (2020). Applied Bayesian Modeling for Assessment of Interpretation Uncertainty in Spatial Domains. Statistics for Data Science and Policy Analysis, 3-13. doi:https://doi.org/10.1007/978-981-15-1735-8_1.

[58] Riquelme, ÁI., Ortiz, JM. (2021). Uncertainty Assessment over any Volume without Simulation: Revisiting Multi-Gaussian Kriging. Math Geosci, 53, 1375-1405. doi:https://doi.org/10.1007/s11004-020-09907-9.

[59] Fouedjio, F., Klump, J. (2019). Exploring prediction uncertainty of spatial data in geostatistical and machine learning approaches. Environ Earth Sci, 78(38). doi:https://doi.org/10.1007/s12665-018-8032-z.

[60] Mery, N., Marcotte, D. (2022). Assessment of Recoverable Resource Uncertainty in Multivariate Deposits Through a Simple Machine Learning Technique Trained Using Geostatistical Simulations. Natural Resources Research, 31, 767-783. doi:https://doi.org/10.1007/s11053-022-10028-9.

[61] Lindi, OT., Aladejare, AE., Ozoji, TM., Ranta, J-P. (2024). Uncertainty Quantification in Mineral Resource Estimation. Natural Resources Research, 33, 2503–2526.

[62] Mery, N., Emery, X., Cáceres, A., Ribeiro, D., Cunha, E. (2017). Geostatistical modeling of the geological uncertainty in an iron ore deposit. Ore Geol Rev, 88, 336-351. doi:https://doi.org/10.1016/j.oregeorev.2017.05.011.

[63] Stephenson, PR., Allman, A., Carville, DP., Stoker, PT., Mokos, P., Tyrrell, J., Burrows, T. (2006). Mineral resource classification - It's time to shoot the 'spotted dog'! Australasian Institute of Mining and Metallurgy Publication Series.

[64] Dumakor-Dupey, NK., Arya, S. (2021). Machine learning—a review of applications in mineral resource estimation. Energies (Basel). doi:https://doi.org/10.3390/en14144079.

[65] Solomatine, DP., Shrestha, DL. (2009). A novel method to estimate model uncertainty using machine learning techniques. Water Resour Res, 45(12). doi:https://doi.org/10.1029/2008WR006839.

[66] Li, T., Xia, Q., Ouyang, Y., Zeng, R., Liu, Q., Li, T. (2024). Prospectivity and Uncertainty Analysis of Tungsten Polymetallogenic Mineral Resources in the Nanling Metallogenic Belt, South China: A Comparative Study of AdaBoost, GBDT, and XgBoost Algorithms. Natural Resources Research, 33, 1049–1071.

[67] Zhao, J., Chi, H., Shao, Y., Peng, X. (2022). Application of AdaBoost Algorithms in Fe Mineral Prospectivity Prediction: A Case Study in Hongyuntan–Chilongfeng Mineral District, Xinjiang Province, China. Natural Resources Research, 31, 2001–2022.

[68] Farhadi, S., Tatullo, S., Boveiri Konari, M., Afzal, P. (2024). Evaluating StackingC and ensemble models for enhanced lithological classification in geological mapping. Journal of Geochemical Exploration, 260, 107441. doi: https://doi.org/10.1016/j.gexplo.2024.107441.

[69] Farhadi, S., Afzal, P., Boveiri Konari, M., Daneshvar Saein, L., Sadeghi, B. (2022). Combination of Machine Learning Algorithms with Concentration-Area Fractal Method for Soil Geochemical Anomaly Detection in Sediment-Hosted Irankuh Pb-Zn Deposit, Central Iran. Minerals, 12(6), 689. doi: https://doi.org/10.3390/min12060689.

[70] Cotrina, M.A., Marquina, J.J., Riquelme, A.I. (2025). Comparison of Machine Learning Techniques for Mineral Resource Categorization in a Copper Deposit in Peru. Natural Resources Research. doi: https://doi.org/10.1007/s11053-025-10505-x.

[71] Desai, C. (2020). Comparative Analysis of Optimizers in Deep Neural Networks. Int J Innov Sci Res Technol 5.

[72] Hassan, E., Shams, MY., Hikal, NA., Elmougy, S. (2023). The effect of choosing optimizer algorithms to improve computer vision tasks: a comparative study. Multimed Tools Appl, 82, 16591-16633. doi:https://doi.org/10.1007/s11042-022-13820-0.

[73] Nanni, L., Maguolo, G., Lumini, A. (2021). Exploiting Adam-like Optimization Algorithms to Improve the Performance of Convolutional Neural Networks. Computer Science.

doi:https://doi.org/https://doi.org/10.48550/arXiv.2103.14689.

[74] Hernández, H., Alberdi, E., Goti, A., Oyarbide-Zubillaga, A. (2023). Application of the k-Prototype Clustering Approach for the Definition of Geostatistical Estimation Domains. Mathematics, 11(3), 740. doi:https://doi.org/10.3390/math11030740.

[75] Bianchi, M., Zheng, C. (2009). SGeMS: A free and versatile tool for three-dimensional geostatistical applications. Ground Water. doi:https://doi.org/10.1111/j.1745-6584.2008.00522.x.

[76] Remy, N. (2005). S-GeMS: The Stanford Geostatistical Modeling Software: A Tool for New Algorithms Development. doi:https://doi.org/10.1007/978-1-4020-3610-1_89.

[77] Ali, Rezaei., Hossein, Hassani., Parviz, Moarefvand., Abbas, Golmohammadi. (2019) Grade 3D Block Modeling and Reserve Estimation of the C-North Iron Skarn Ore Deposit, Sangan, NE Iran. Global Journal of Earth Science and Engineering, 6(2019). doi:https://doi.org/10.15377/2409-5710.2019.06.4.

[78] Heuvelink, GBM., Pebesma, EJ. (2002). Is The Ordinary Kriging Variance A Proper Measure Of Interpolation Error? The fifth international symposium on spatial accuracy assessment in natural resources and environmental sciences.

[79] da Silva, CZ., Nisenson, J., Boisvert, J. (2022). Grade Control with Ensembled Machine Learning: A Comparative Case Study at the Carmen de Andacollo Copper Mine. Natural Resources Research, 31, 785-800. doi:https://doi.org/10.1007/s11053-022-10029-8.

[80] Tülay., BAYRAMİN, T. (2016). Assessment of ınverse distance weighting (ıdw) ınterpolation on spatial variability of selected soil properties in the Cukurova plain. Tarım Bilimleri Dergisi. doi:https://doi.org/10.1501/tarimbil_0000001396.

[81] Estrada-Gil, JK., Fernández-López, JC., Hernández-Lemus, E., Silva-Zolezzi, I., Hidalgo-Miranda, A., Jiménez-Sánchez, G., Vallejo-Clemente, EE. (2007). GPDTI: A genetic programming decision tree induction method to find epistatic effects in common complex diseases. Bioinformatics. doi:https://doi.org/10.1093/bioinformatics/btm205.

[82] Marinos, V., Marinos, P., Hoek, E. (2005). The geological strength index: Applications and limitations. Bulletin of Engineering Geology and the Environment. doi:https://doi.org/10.1007/s10064-004-0270-5.

[83] Emery, X. (2009). The kriging update equations and their application to the selection of neighboring data. Comput Geosci, 13, 269-280. doi:https://doi.org/10.1007/s10596-008-9116-8.

[84] Adhikary, SK., Muttil, N., Yilmaz, AG. (2016). Genetic Programming-Based Ordinary Kriging for Spatial Interpolation of Rainfall. J Hydrol Eng, 21(2). doi:https://doi.org/10.1061/(asce)he.1943-5584.0001300.

[85] Marquina-Araujo, JJ., Cotrina-Teatino, MA., Cruz-Galvez, JA., Noriega-Vidal, EM., Vega-Gonzalez, JA. (2024). Application of Autoencoders Neural Network and K-Means Clustering for the Definition of Geostatistical Estimation Domains. Mathematical Modelling of Engineering Problems, 11,1207–1218.

[86] Dorman, KS., Maitra, R. (2022). An efficient k-modes algorithm for clustering categorical datasets. Stat Anal Data Min. doi:https://doi.org/10.1002/sam.11546.

[87] Marquina, J., Cotrina, M., Mamani, J., Noriega, E., Vega, J., Cruz, J. (2024). Copper Ore Grade Prediction using Machine Learning Techniques in a Copper Deposit. Journal of Mining and Environment, 15,1011–1027.

[88] Cotrina, M., Marquina, J., Mamani, J., Arango, S., Gonzalez, J., Ccatamayo, J., Noriega E. (2024). Predictive model using machine learning to determine fuel consumption in CAT-777F mining equipment. Int J Min Miner Eng, 15, 147–160.

[89] Cotrina, M., Marquina, J., Noriega, E., Mamani, J., Ccatamayo, J., Gonzalez, J., Arango, S. (2024). Predicting Open Pit Mine Production using Machine Learning Techniques: A Case Study in Peru. Journal of Mining and Environment, 15, 1345–1355.

[90] Joseph, FJJ., Nonsiri, S., Monsakul, A. (2021). Keras and TensorFlow: A Hands-On Experience. EAI/Springer Innovations in Communication and Computing. doi:https://doi.org/10.1007/978-3-030-66519-7_4.

[91] Kingma, DP., Ba, JL. (2015). Adam: A method for stochastic optimization. 3rd International Conference on Learning Representations, ICLR 2015 - Conference Track Proceedings.

[92] Elshamy, R., Abu-Elnasr, O., Elhoseny, M., Elmougy, S. (2023). Improving the efficiency of RMSProp optimizer by utilizing Nestrove in deep learning. Sci Rep, 13, 8814.

[93] Tian, Y., Zhang, Y., Zhang, H. (2023). Recent Advances in Stochastic Gradient Descent in Deep Learning. Mathematics, 11, 682.

[94] Lydia, AA., Francis, FS. (2019). Adagrad - An Optimizer for Stochastic Gradient Descent. INTERNATIONAL JOURNAL OF INFORMATION AND COMPUTING SCIENCE 6.

[95] Yacouby, R., Axman, D. (2020). Probabilistic Extension of Precision, Recall, and F1 Score for More Thorough Evaluation of Classification Models. doi:https://doi.org/10.18653/v1/2020.eval4nlp-1.9.

[96] Dalianis, H. (2018). Evaluation Metrics and Evaluation. Clinical Text Mining. doi:https://doi.org/10.1007/978-3-319-78503-5_6.